Consequence of Flow Nonuniformity on the Measurement of Effective Diffusivity

Measurements of effective diffusivity by the chromatographic method are shown to be biased by nonuniformity of the external porosity in a cross-section of the column. A very simple model is proposed to interpret experimental results. A modified Van Deemter method is given to extract the axial dispersion and effective diffusion coefficients from chromatographic peaks. This method allows one to ignore the external porosity distribution. Experiments show that even though axial dispersion obeys classical correlations, the internal mass transfer parameters may be strongly affected by the external porosity distribution.

L. C. Cui
D. Schweich
J. Villermaux
Laboratoire des Sciences
du Génie Chimique
CNRS-ENSIC
BP 451, 1 rue Grandville, 54001
Nancy cedex, France

Introduction

The chromatographic method is used frequently for measuring effective diffusivities; however, some anomalous results are reported in the literature. Among these, the strangest is the variation of the effective diffusion coefficient with fluid flow rate (Kehinde et al., 1983; Cheng et al., 1984; Rodrigues et al., 1982). One of the most striking results was reported by Hsu and Haynes (1981) who found that diffusion in microcrystals of zeolite seems to be affected by the flow rate! The latter authors attributed their results to a slight nonlinearity of the adsorption isotherm which was responsible for unreliable estimates of the effective diffusivity.

There are two possible explanations for this flow-rate dependence: it can be due to either a physical process or a bias introduced by the parameter-estimation procedure. As a possible physical process, Rodrigues et al. (1982, 1988) proposed forced convection inside the porous particle. As pointed out by Rodrigues (1982, 1988) and Cresswell and Orr (1982), this explanation is plausible only in large pore catalyst (diameter larger than 10^4 Å). Gangwal et al. (1978), Cresswell and Orr (1982), Villermaux and Antoine (1978), and Boersma-Klein and Moulijn (1979) have shown that correlation between parameters may yield erroneous estimates of internal diffusion coefficients and artificial dependence on other parameters. Most of the previous authors conclude that an accurate *a-priori* estimate of axial dispersion is absolutely necessary to obtain reliable results. Any uncertainties in coefficients of the axial dispersion and external mass transfer processes are reflected on the parameter of the internal mass transport process, unless the contribution of the former processes can be shown to be negligible. If the latter condition can be met for external mass transfer limitation, it is scarcely met for axial dispersion.

Estimating axial dispersion seems to be hazardous as shown by many researchers (Ahn et al., 1986; Tostas and Schlünder, 1988; Hsiang and Haynes, 1977; Carbonell, 1980), proving that packing heterogeneity may be responsible for large discrepancies with respect to known empirical correlations. It is also known that packing heterogeneity is able to explain anomalous external mass or heat transfer coefficients (Martin, 1978; Schlünder, 1978).

We are going to show that external porosity heterogeneity can be responsible for biased estimates of internal diffusivity. This is especially important in the chromatographic measurement method where low column diameter/particle diameter ratios are used.

Chromatographic Column Model with Nonuniform Extragranular Porosity

Presently, a chromatographic column can be mathematically represented either by a continuous or a staged model. In continuous models, the dispersion process is accounted for by Fick's law. This approach holds provided that the fluctuations of fluid velocity are correlated on a scale much smaller than the characteristic lengths of the porous medium (Hughes and Prager, 1983). The correlation is measured by the particle Péclet number which can be interpreted as the ratio of the particle diameter to a dispersion correlation length. In the mechanical dispersion regime, the radial Péclet number is of the order of 5 to 10 in the gas phase (Gunn, 1987). As a consequence, for column diameter/particle diameter ratios smaller than 10, the radial dispersion process cannot be properly accounted for by Fick's law because velocity fluctuations are correlated over 10 particle diameters.

Staged models can be used to overcome this problem. This

type of model is soundly based on the theory of random walks originating in theoretical physics (Hughes and Prager, 1983). The column is thus modeled by a suitable network of mixing cells and the number of cells being related to the Péclet numbers, as will be discussed later. The proposed model is an extension of the well-known mixing cells-in-series model (Villermaux, 1987). The column is assumed to be composed of J/N elementary blocks in series (Figure 1). Each block is composed of n lines in parallel, and each line is composed of a series of N mixing cells. The volume fraction, the void fraction, and the volumetric flow rate may be different from line to line, but blocks in the series and cells in a line are assumed to be identical.

Along a given line, there are J mixing cells from the inlet to the outlet of the column. According to the equivalence between the mixing cell model and the dispersion model, J accounts for the axial dispersion process, L being the column length and d_p the particle diameter, J is of the order of L/d_p in the mechanical dispersion regime. Complete mixing of the outlet streams of the parallel lines occurs at the end of a block. This means that LN/J is a characteristic radial dispersion length. In the mechanical regime. LN/J is of the order of a few times the particle diameter d_p (Gunn, 1987). Finally, the number of parallel lines can be expected to be close to d_c/d_p. Martin (1978), Schlünder (1978), and Ahn et al. (1986) have used a similar model although they have neglected the radial transfer process.

The chromatographic process will be described under the following assumptions:

- Temperature, pressure, and volumetric flow rate are constant.
- Solid/fluid equilibrium is linear.
- Mass transfer limitations are accounted for by an equivalent first-order dynamical system (Villermaux, 1987).
- According to Villermaux, the transfer function of line k of a block is given by:

$$g_k(s) = (1 + s\tau_{0k}[1 + M_k(s)])^{-N} \tag{1}$$

where τ_{0k} is the mean residence time in the void fraction of one cell of line k, and $M_k(s)$ is the particle transfer function accounting for sorption dynamics. Let ϵ_k be the external porosity in line k:

$$M_k(s) = \frac{1 - \epsilon_k}{\epsilon_k} \frac{\alpha}{1 + t_{mk}s} \tag{2}$$

α is the partition coefficient, and t_{mk} the overall mass transfer time. α is composed of two additive contributions: the first the internal porosity of the porous particle and the second the adsorption coefficient. For an inert tracer, α reduces to the internal porosity, and thus α never vanishes except for a nonporous particle.

Let x_k be a fraction of the flow rate in line k. The transfer function of a block is:

$$G_1(s) = \sum_{k=1}^{n} x_k g_k(s) \tag{3}$$

Finally, the transfer function of the whole column is:

$$G(s) = G_1(s)^{J/N} \tag{4}$$

Many properties of chromatograms are obtained from the mean retention time and from the variance. Using Van der Laan's theorem (1958) and the above equations, one obtains:

$$t_R = t_0(1 + K') \tag{5}$$

where t_R is the retention time, t_0 the mean residence time of the fluid in the external porous volume of the column, and K' the capacity factor. Letting ϵ be the mean external porosity, then:

$$K' = \frac{1 - \epsilon}{\epsilon} \alpha \tag{6}$$

$$t_0 = \frac{\epsilon V}{Q} \tag{7}$$

If λ_k is the volume fraction of the column occupied by line k, the mean porosity is given by:

$$\epsilon = \sum_{k=1}^{n} \lambda_k \epsilon_k \tag{8}$$

The peak variance is then found to be:

$$\frac{\sigma^2}{t_R^2} = \frac{(N+1)\sum_{k=1}^{n} \frac{\lambda_k^2}{x_k}\left[\frac{\epsilon_k + (1-\epsilon_k)\alpha}{\epsilon + (1-\epsilon)\alpha}\right]^2 - N}{J} + \frac{2K'}{1+K'} \frac{\sum_{k=1}^{n} \left(\frac{1-\epsilon_k}{1-\epsilon}\right)\lambda_k t_{mk}}{t_R} \tag{9}$$

For the classical model accounting for uniform porosity (single line), Eq. 9 reduced to the well-known formula:

$$\frac{\sigma^2}{t_R^2} = \frac{1}{J} + \frac{2K'}{1+K'} \frac{t_m}{t_R} \tag{10}$$

As usual, the peak variance is composed of two additive contributions: one reflecting dispersion (first term in the righthand

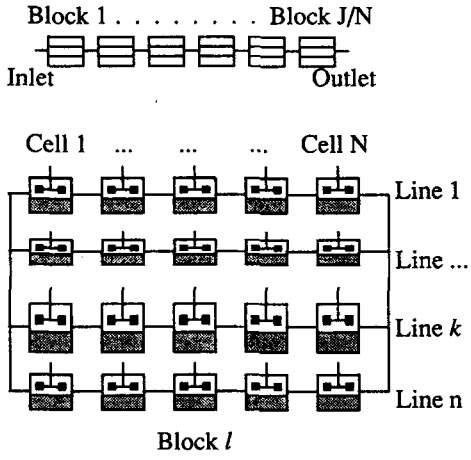

Figure 1. GC column modeled by a series of blocks composed of several lines in parallel.

side of Eq. 9) and one reflecting mass transfer. However, Eq. 9 shows that the "dispersion" contribution depends on the partition coefficient α, contradicting Eq. 10.

Determining the Mass Transfer Time by Van Deemter's Method

From an experimental point of view, it is impossible to determine ϵ_k, λ_k, and x_k. Consequently, the proposed model involves too many adjustable parameters, and it would be hazardous to fit experimental curves. Van Deemter's method avoids this problem. Knowing the mean retention time and reduced variance of the chromatographic peaks, the true mass transfer time t_m can be determined by the method described below.

In order to get the mass transfer time from the peak variance, one must first determine the dispersion contribution. This may be done by chromatographic experiments using nonporous and nonadsorbing ($\alpha = 0$) particles. In the latter case, Eq. 9 becomes:

$$\frac{\sigma^2}{t_R^2} = \frac{1}{J_0^*} \tag{11a}$$

$$J_0^* = \frac{J}{(N+1)\sum_{k=1}^{n} \frac{\lambda_k^2}{x_k}\left[\frac{\epsilon_k}{\epsilon}\right]^2 - N} = J/\psi \tag{11b}$$

J_0^* is a lumped dispersion parameter accounting for axial and radial dispersion and the velocity profile. It is readily obtained from experimental curves with nonporous particles. It can be shown that J is the upper bound to J_0^*. Moreover, if the mean residence time of the fluid is the same in each line ($\lambda_k \epsilon_k / x_k = \epsilon$), then $J_0^* = J$. This means that the axial dispersion coefficient thus calculated is independent of the external porosity distribution in the latter case. In other words, there exist some experimental conditions under which the dispersion process is not affected by the external porosity distribution. Assuming that axial dispersion is identical in the columns packed with the porous and the nonporous particles, an effective mass transfer time t_m^* is obtained from experimental variance by substracting the dispersion contribution previously determined:

$$\frac{2K'}{1+K'}\frac{t_m^*}{t_R} = \frac{\sigma^2}{t_R^2} - \frac{1}{J_0^*} \tag{12}$$

Combining Eqs. 9, 11a, 11b and 12 enables one to interpret t_m^* in terms of nonuniform porosity distribution:

$$t_m^* = \sum_{k=1}^{n}\left(\frac{1-\epsilon_k}{1-\epsilon}\right)\lambda_k t_{mk} + \frac{t_R}{J_0^*}\frac{1+K'}{2K'}\phi \tag{13a}$$

$$\phi = \frac{(N+1)\sum_{k=1}^{n}\frac{\lambda_k^2}{x_k}\left[\left(\frac{\epsilon_k + (1-\epsilon_k)\alpha}{\epsilon + (1-\epsilon)\alpha}\right)^2 - \left(\frac{\epsilon_k}{\epsilon}\right)^2\right]}{(N+1)\sum_{k=1}^{n}\frac{\lambda_k^2}{x_k}\left[\frac{\epsilon_k}{\epsilon}\right]^2 - N} \tag{13b}$$

In the general case, Eq. 13a shows that t_m^* depends on the flow rate owing to t_{mk} and t_R. When the external mass transfer resistance is negligible, t_{mk} becomes independent of k, and Eq. 13a shows that the effective mass transfer time t_m^* depends linearly on the retention time due to the correction factor ϕ. Let us emphasize that α never vanishes for porous particles, even for an inert tracer, so that ϕ never vanishes except for a uniform external porosity distribution. Equation 12 is identical to Eq. 10 after substitution of J_0^* and t_m^* for J and t_m. This means that J_0^* and t_m^* would be the dispersion and mass transfer parameters which were determined assuming uniform porosity in the column. From Eqs. 13a and 13b, it is concluded that:

1. t_m^* is a biased measure of the mass transfer time when there is a nonuniform external porosity distribution.
2. The second term of Eq. 13a accounting for the dependence upon the volumetric flow rate, is a function of the partition coefficient α.

As stated above, J_0^* and t_m^* can be deduced from the experimental variances of chromatographic peaks obtained with nonporous and porous particles. Owing to the statistical weight of noise in tails of chromatographic peaks, these determinations can be inaccurate. An alternative method consists of fitting the experimental curves with the model assuming uniform porosities. With the nonporous particles, J_0^* is the only adjustable parameter. Knowing J_0^*, t_m^* is the only adjustable parameter fitted on the curves obtained with porous particles. This method avoids simultaneous fitting of several parameters and yields accurate results.

Experimental example

Internal mass transfer in a microporous alumina (GCO 70, Rhône-Poulenc) was studied by the chromatographic method. Table 1 summarizes the properties of the column and of the alumina particles. Pulses of various tracers were injected into the column, and the response was recorded with a microcomputer. To obtain the contributions of the input signal and extra-column phenomena (injector, detector, and unions), identical experiments without the chromatographic column were performed under the same experimental conditions. The latter experiments may be considered to yield the equivalent input signals into the column in the former experiments.

In earlier studies, the dispersion parameter was obtained either from empirical correlations or from experiments with the

Table 1. Column and Packing Characteristics

Column	
Length: 1 m	
Internal diameter: $4.55\ 10^{-3}$ m	
External porosity: 0.49	
Temperature: 20°C	
Operating pressure: 1 atm	
Carrier gas: He, Ar	
Tracer: He, Ar, N_2, CH_4	
Alumina (Spherical Pellets)	
GCO 70 Rhône-Poulenc	
Diameter: $2.0\ 10^{-3}$ m	
Internal porosity: 0.627	
Mean pore radius: 10^{-8} m	
Surface area: 200 mg^2/g	
Tracer	Capacity factor K'
He	0.845
Ar	1.03
N_2	1.04
CH_4	1.29

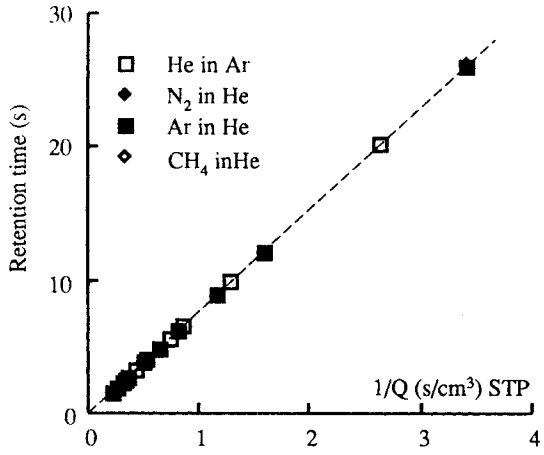

Figure 2. Retention time of various tracers vs. reciprocal of flow rate (20°C, 0.1 MPa) on the alumina impregnated with glycerol.
Most data points are superimposed.

same column packed with a nonporous adsorbent (glass beads) as similar as possible to the porous adsorbent. Unfortunately, empirical correlations are not very accurate and the dispersion parameter can hardly be determined with less than 10% uncertainty. To avoid this problem, we performed the dispersion measurement and the mass transfer measurement on the same packing. After the series of experiments with the porous alumina, the internal porosity was filled with glycerol to obtain a nonporous, nonadsorbing packing. The detailed impregnation technique is described by Cui (1989). A new series of chromatographic experiments was performed on this impregnated alumina to determine axial dispersion as a function of flow rate.

The classical model assuming uniform porosity, was used to fit the experimental curves and to obtain J_0^* and t_m^* as described in the previous section. The resulting values of the parameters are illustrated on Figures 2 to 5. The slope of the straight line in Figure 2 yields the external volume accessible to the fluid outside the impregnated alumina. It is found to be independent of the tracer, showing that alumina actually behaves as a nonsorbing material. This volume ($7.72\ 10^{-6}$ m^3) is within 3% of the volume deduced from the weight of alumina in the column. Figure 3 shows the particle Peclet number which is related to J_0^* by (Villermaux, 1987):

$$Pe_p = \frac{ud_p}{D_{ax}} = 2J_0^* \frac{d_p}{L} \tag{14}$$

Data points approximately agree with the classical correlation of Edwards and Richardson (1970). This suggests that the correction factor ψ in Eq. 11b is close to 1. From Eq. 5, the capacity factor K' is deduced from the mean residence times measured on the porous particles. Figure 4 illustrates the mean residence time of the tracers. From Eq. 5, capacity factors are deduced from the slopes of the straight lines. They are listed in Table 1. Then, using the value of J_0^* obtained from the experiments on the impregnated alumina, the mass transfer time t_m^* was fitted. In Figure 5, the mass transfer time t_m^* is plotted against $(1 + K')t_R/2K'J_0^*$. By means of a correlation by Wakao and Funazkri (1978), the external mass transfer time is found to be negligible with respect to t_m^*. Consequently, Eq. 13a reduces to:

$$t_m^* = t_i + \frac{t_R}{J_0^*} \frac{1 + K'}{2K'} \phi \tag{15}$$

where t_i is the internal mass transfer time. Equation 15 suggests a linear dependence of t_m^* on t_R which is readily observed in Figure 5. Assuming instantaneous adsorption equilibrium, t_i is given by:

$$t_i = t_D = \frac{\alpha d_p^2}{60 D_e''} \tag{16}$$

where D_e'' is the effective internal diffusion coefficient in the fluid of the pores of the alumina particle. Linear regressions on the data points of Figure 5 give the parameters ϕ_{exp}, t_i and D_e'' listed in Table 2. We note that because of the microporous structure of the alumina (see Table 1), the Knudsen regime prevails. As expected, the diffusion coefficients, D_e'', are roughly proportional to the reciprocal of the square root of the tracer molecular weight.

Interpreting the ϕ factor would be hazardous because of scattering of data points in Figure 5. Consequently, we tried to pre-

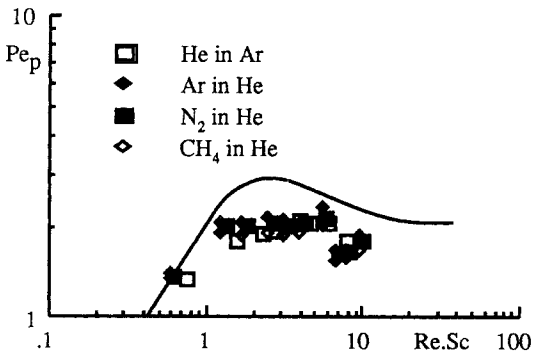

Figure 3. Particle Peclet number vs. *Re.Sc* on the impregnated alumina packing.
Continuous curve is the Edwards-Richardson correlation.

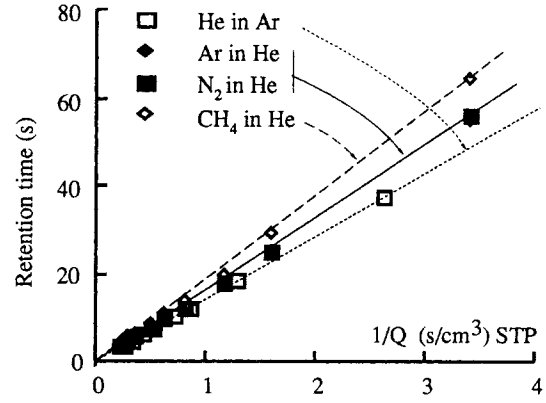

Figure 4. Retention time of various tracers vs. reciprocal of flow rate (20°C, 0.1 MPa) on the porous alumina.
The slope of the straight lines gives the capacity factor K'.

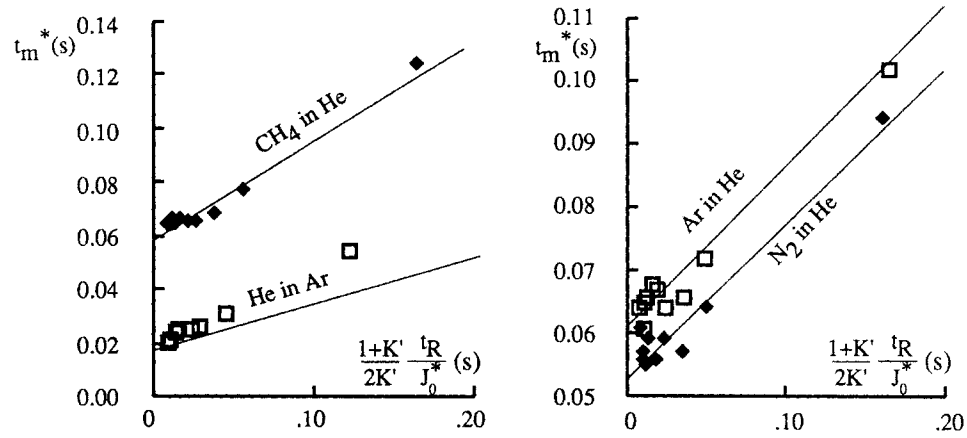

Figure 5. Effective internal mass transfer time vs. corrected retention time.

Data points are obtained by Van Deemter method. Straight lines are prediction of the flow-rate dependence according to the parameters in last line of Table 2 and $N = 2$.

dict ϕ, assuming that the column can be modeled by two parallel lines. Since the column diameter is a little larger than $2d_p$, one line is assumed to be composed of a compact packing of alumina spheres equivalent to a column of diameter $2d_p$. The second line is the void annulus necessary to obtain the actual column volume. This simplified approach is similar to that of Martin (1978) or Ahn et al. (1986). The volume fraction of the two lines are thus:

$$\lambda_1 = 4\left(\frac{d_p}{d_c}\right)^2, \quad \lambda_2 = 1 - \lambda_1 \tag{17}$$

The void fraction ϵ_2 in line 2 is 1. The void fraction in line 1 is deducted from the overall experimental porosity ϵ (see Table 1):

$$\epsilon_1 = 1 - (1 - \epsilon)/\lambda_1 \tag{18}$$

Since there are two particles at most in the cross-section of the column, one may assume that the radial dispersion length is of the order of $2d_p$. The axial particle Peclet number being close to 2, the axial dispersion length is of the order of d_p. Consequently, we may assume that complete radial mixing occurs over two particles and thus the number of mixing cells per line of a block, N, is close to 2. Contrary to other model parameters, there is no *a priori* estimate of x_1. Using the estimations above and Eq. 9, only x_1 was fitted to predict the 38 experimental data points of Figure 5. The best fit is illustrated by the straight lines of Figure 5. Finally, ϕ was deduced (ϕ_{est}) for each couple of gas from the best x_1. Table 2 shows the results for two values of N to illustrate the sensitivity of ϕ to this parameter. For $N = 2$, the ϕ factors are strikingly similar to those coming from experiments except for helium tracer in argon carrier. Using the parameters of Table 2 and Eqs. 11a and 11b gives the ψ factor which relates the true axial dispersion parameter J to the effective dispersion parameter J_0^*. ψ is found to be 1.07 indicating that dispersion is practically unaffected by the nonuniform external porosity distribution as already shown by Figure 3. We note that changing N from 2 to 5 does not result in a dramatic change. This means that an accurate determination of N is not necessary, at least under our experimental conditions.

The above results show that J_0^* and t_m^* can be used to interpret the chromatographic peaks. However, J_0^* and t_m^* have been measured by fitting the experimental curves with the model assuming uniform porosity. It remains to be seen that this model is able to represent the peaks, although there is a nonuniform porosity. It is well known that by an appropriate choice of the unknown parameters it is easy to fit any experimental curve. Therefore, we shall only compare theoretical curves having the same mean and variance, assuming either nonuniform or uniform external porosity. The parameters of the model accounting for nonuniform porosity are given in Table 3; they correspond to an injection of CH_4 in He as indicated in Table 2. Using Eqs. 15

Table 2. Internal Mass Transfer and Model Parameters

Tracer/carrier	ϕ_{exp}	$t_i(s)$	D_e'' (m^2/s)	ϕ_{est} $N = 2$	ϕ_{est} $N = 5$
He/Ar	0.29	0.0189	$2.86\ 10^{-6}$	0.17	0.12
Ar/He	0.25	0.0611	$1.08\ 10^{-6}$	0.25	0.24
N_2/He	0.24	0.0535	$1.25\ 10^{-6}$	0.25	0.25
CH_4/He	0.38	0.0591	$1.40\ 10^{-6}$	0.36	0.41
$\lambda_1 = 0.773$ $\lambda_2 = 0.227$		$\epsilon_1 = 0.34$	$\epsilon_2 = 1.0$ $x_1 =$	0.61	0.63

Table 3. Simulation Data for Figure 6*

	Uniform Porosity Single Line	Heterogeneous Porosity 2 Lines, 2 Cells/Block
$t_0(s)$	10	10
$t_i(s)$	0.059	0.059
$t_m(s)$	0.0755	0.059
J	467	500
K'	1.29	1.29
λ_1	1	0.773
ϵ_1	0.49	0.34
ϵ_2	—	1.0
x_1	1	0.61
ϕ	0	0.38
ψ	1	1.066

*Parameters correspond to CH_4 in He as listed in Table 2.

and 11, the effective J_0^* and t_m^* parameters of the uniform model were calculated (Table 3). Finally, the responses to a Dirac pulse were calculated and illustrated in Figure 6 as two indistinguishable peaks. This proves that, under the chosen experimental conditions, either the nonuniform or uniform model is able to fit the experimental curves equally. Three conclusions can be drawn from Figure 6.

1. Good fit with a uniform model does not allow to discard a possible porosity distribution. This may explain why the possible effect of nonuniform porosity has been overlooked until now.

2. The classical uniform model can be used to fit the experimental curves and to obtain the apparent parameters t_m^* and J_0^*, and finally t_m as explained above. Let us emphasize that the uniform model can fail to predict the experimental curves, although this was not the case in our study.

3. Only the deformation of experimental curves as a function of flow rate (i.e., retention times) enables one to detect the bias introduced by the porosity distribution.

Finally, it is concluded from Eq. 15 that the internal mass transfer time t_i is the limiting value of t_m^* at zero retention time or infinite flow rate. This property and the modified Van Deemter method described above would allow one to reinterpret previously published results in light of the proposed approach.

Discussion

The model presented above explains very simply the variation of the internal mass transfer time or effective diffusion coefficient with flow rate. Convection inside the porous particle or anomalously-slow external mass transfer could also explain the results. Internal convection can be rejected since the alumina studied is microporous. External mass transfer contribution has also been rejected on the basis of the correlations available to estimate mass transfer coefficients. However, for low Reynolds numbers, these correlations seem questionable: external mass transfer coefficient could be several orders of magnitude smaller than predicted. Nelson and Galloway (1975) have proposed a theoretical explanation showing that external mass transfer coefficient should go to zero when Reynolds number goes to zero contrary to classical correlations.

1. This explanation is hazardous because it is based on surface renewal theory which is questionable at low Reynolds number.

2. The experimental results presented in this study could not be represented in terms of the Nelson-Galloway correlation (Cui 1989).

On the other hand, assuming classical correlations for external mass transfer to be valid, Martin (1978) and Schlünder (1978) have shown that anomalously-low apparent external mass transfer coefficients may result from flow heterogeneity. As a consequence, in order to preserve coherence among our assumptions, classical correlations for external mass transfer have been assumed to hold. This is not a serious limitation to our conclusions as the external mass transfer time is found negligible under our experimental conditions using such correlations.

Flow heterogeneity in a cross-section of a column seems to be now the common explanation for three independent observations: anomalous external mass transfer coefficients (Martin, 1978; Schlünder, 1978); anomalous axial dispersion (Hsiang and Haynes, 1977; Carbonell, 1980; Tsotas and Schlünder, 1988; Ahn et al., 1986) and flow-rate-dependent internal diffusion coefficient (this paper). This unique physical process resulting in three different consequences gives support to the approach. Although both axial dispersion and apparent internal mass transfer are flow-rate-dependent in the general case, the example presented above shows that axial dispersion seems to be normal whereas internal mass transfer is flow-rate-dependent. It turns out that the reliability of the Single Pellet String Reactor (SPSR) described by Scott et al. (1974) becomes questionable. The latter authors concluded from an analysis of axial dispersion and pressure drop that, for a d_c/d_p ratio from 1.1 to 1.4, the flow behavior is very similar to that in conventional packed beds. Our results show that this may be a coincidence, at least for axial dispersion. Although the intraparticle convection effect in large pore catalyst described by Rodrigues et al. (1982) is well established, the experimental results should be reconsidered since the authors have worked with a SPSR. Since they obtained tortuosity factors as high as 80 and permeability coefficients far from reasonable values, it is possible that part of their observation may be explained by the nonuniform external porosity.

Finally, the dependence of the correction factors ϕ and ψ on the partition coefficient is an interesting property. The study of tracers of variable retention property might give further insight into the consequence of the velocity distribution.

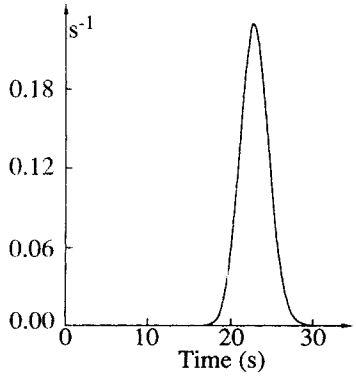

Figure 6. Comparison between the models accounting for heterogeneous and homogeneous external porosity in a cross-section.

Simulation parameters (Table 3) typical of an injection of CH_4 in He. Two normalized chromatograms are superimposed in the figure.

Acknowledgment

Rhône Poulenc Company is gratefully acknowledged for supplying the alumina and the physical characteristics.

Notation

D_{ax} = axial dispersion coefficient
D_e'' = effective internal diffusion coefficient
d_c = column diameter
d_p = particle diameter
g_k = transfer function of block k
G_l = transfer function of line l
G = transfer function of the column
J = number of cells in a line
J_0^* = apparent number of mixing cells in series for an unretained solute
k = line number
K' = capacity factor
L = column length

M_k = particle transfer function
N = number of cells in a line of a block
Pe_p = particle Péclet number
t_D = internal diffusion time
t_i = internal mass transfer time
t_m = mean overall mass transfer time
t_m^* = apparent mean overall mass transfer time
t_{mk} = overall mass transfer time in line k
t_R = mean retention time
t_0 = mean retention time in the external porosity
u = fluid velocity
x_k = fraction of flow rate in line k

Greek letters

α = partition coefficient
ϵ_k = external porosity in line k
ϵ = mean external porosity
ϕ = correction factor defined by Eq. 13b
λ_k = volume fraction occupied by line k
ψ = correction factor defined by Eq. 11
σ^2 = peak variance
τ_{0k} = mean residence time in the void fraction of one cell of line k

Literature Cited

Ahn, B. J., A. Zoulalian, and J. M. Smith, "Axial Dispersion in Packed Beds with Large Wall Effect," *AIChE J.*, **32**(1), 170 (1986).

Boersma-Klein, W., and J. A. Moulijn, "Evaluation in Time Domain of Mass Transfer Parameters from Chromatographic Peaks," *Chem. Eng. Sci.*, **34**, 959 (1979).

Carbonell, R. G., "Flow Nonuniformities in Packed Beds: Effects on Dispersion," *Chem. Eng. Sci.*, **35**, 1347 (1980).

Cheng, S., A. Rodrigues, and A. Zoulalian, "Diffusivity Measurements in Large Pore Catalysts by a Dynamic Chromatographic Technique," *Ibero Amer. Symp. on Catalysis*, Lisbon, Portugal (1984).

Cresswell, D. L., and N. H. Orr, "Measurement of Binary Gaseous Diffusion Coefficients within Porous Catalysts," *Residence Time Theory in Chemical Engineering*, Pethö and Noble, eds., Verlag Chemie, 41 (1982).

Cresswell, D. L., "Intraparticle Convection: Its Measurement and Effect on Catalyst Activity and Selectivity," *Appl. Cat.*, **15**, 103 (1985).

Cui, L. C., "Diffusivité Effective en Chromatographie et en Catalyse: Signification, Mesure et Interprétation," PhD Thesis, Institut National Polytechnique de Lorraine, Nancy, France (1989).

Edwards, M. F., and J. F. Richardson, "The Correlation of Axial Dispersion Data," *Can. J. Chem. Eng.*, **48**, 466 (1970).

Gangwal, S. K., R. R. Hudgins, and P. L. Silveston, "Conditions Needed for Satisfactory Measurement of Mass Transfer Coefficients, Internal Diffusivity and Adsorption Rate Constants," *Can. J. Chem. Eng.*, **56**, 554 (1978).

Gunn, D. J., "Axial and Radial Dispersion in Fixed Beds," *Chem. Eng. Sci.*, **42**,(2), 363 (1987).

Hsiang, T. C., and H. W. Haynes, "Axial Dispersion in Small Diameter Beds of Large Spherical Particles," *Chem. Eng. Sci.*, **32**, 678 (1977).

Hsu, L. K. P., and H. W. Haynes, "Effective Diffusivity by the Gas Chromatography Technique: Analysis and Application to Measurement of Diffusion of Various Hydrocarbons in Zeolite NaY," *AIChE J.*, **27**(1), 81 (1981).

Hughes, B. D., and S. Prager, "Random Processes and Random Systems: an Introduction," *The Mathematics and Physics of Disordered Media*, B. D. Hughes and B. W. Ninham, eds., Springer Verlag, Berlin (1983).

Kehinde, A. J., R. R. Hudgins, and P. Silveston, "Measurement of Mass Transfer in Packed Beds at Low Reynolds Numbers by Imperfect Pulse Chromatography," *J. Chem. Eng. Japan*, **16**(6), 483 (1983).

Martin, H., "Low Peclet Number Particle to Fluid Heat and Mass Transfer in Packed Beds," *Chem. Eng. Sci.*, **33**, 913 (1978).

Nelson, P. A., and T. R. Galloway, "Particle to Fluid Heat and Mass Transfer in Dense Systems of Fine Particles," *Chem. Eng. Sci.*, **30**, 1 (1975).

Rodrigues, A. E., B. J. Ahn and A. Zoulalian, "Intraparticle Forced Convection Effect in Catalyst Diffusivity Measurements and Reactor Design," *AIChE J.*, **28**,(4), 541 (1982).

Rodrigues, A. E., and R. M. Quinta Ferreira, "Convection, Diffusion and Reaction in a Large Pore Catalyst Particle," *AIChE Symp. Ser.*, **84**, 266 (1988).

Schlünder, E. U., "Transport Phenomena in Packed Bed Reactors," *ACS Symp. Ser.* No. 72, 110, Chemical Reaction Engineering Reviews, Houston (1978).

Scott, D. S., Wey Lee, and J. Papa, "The Measurement of Transport Coefficient in Gas-Solid Heterogeneous Reactions," *Chem. Eng. Sci.*, **29**, 2155 (1974).

Tsotas, E., and E. U. Schlünder, "On Axial Dispersion in Packed Beds with Fluid Flow," *Chem. Eng. Process.*, **24**, 15 (1988).

van der Laan, E.Th., "Notes on the Diffusion-Type Model for the Longitudinal Mixing in Flow," *Chem. Eng. Sci.*, **7**, 187 (1958).

Villermaux, J., and B. Antoine, "Construction et Ajustement des Modèles Mathématiques: une Science ou un Art?, *Bull. BRGM, III(4), 327* (1978).

Villermaux, J., "Chemical Engineering Approach to Dynamic Modeling of Linear Chromatography," *J. of Chrom.*, **406**, 11 (1987).

Wakao, N., and T. Funazkri, "Effect of Fluid Dispersion Coefficients on Particle to Fluid Mass Transfer Coefficients in Packed Beds," *Chem. Eng. Sci.*, **33**, 1375 (1978).

Manuscript received May 24, 1989, and revision received Nov. 7, 1989.